

Using continuous control for amplification and displacement of chaotic signals

J.M. González-Miranda^a

Departamento de Física Fundamental, Universidad de Barcelona, avenida Diagonal 647, 08028 Barcelona, Spain

Received: 11 March 1998 / Revised: 9 July 1998 / Accepted: 13 July 1998

Abstract. Continuous control, used on chaotic systems that bear some special symmetries, gives rise to interesting generalized synchronization behaviors which include modification of signal amplitudes, and trajectories of the system being controlled that reproduce the controller attractor in a region of phase space out of the region where it is stable. Theoretical reasoning and computer simulations show how continuous control methods can be used to obtain these generalized synchronization behaviors, and to tune the desired degree of amplification or displacement. Moreover it is shown that these behaviors can be asymptotically stable, and very robust against external noise and mismatches in the controlling arrangement.

PACS. 05.45.+b Theory and models of chaotic systems

1 Introduction

The study of chaotic driving has emerged, during the last years, as an object of major attention in the field of study of the theories and models of chaotic systems. The situations considered are those in which a chaotic system, called the drive, provides a signal which acts on another chaotic system, called the response. A significant contribution has been the report by Pecora and Carroll [1] of a driving method under which two identical chaotic systems may be synchronized. This means that the distance between the two systems in phase space converges to zero when one of them acts as the drive and the other as the response. Several authors have proposed modifications of the Pecora and Carroll method for specific purposes [2–5], while others have proposed to use control of chaos techniques as an alternative to the Pecora and Carroll and related synchronization methods. In particular, Ding and Ott [6] and Kapitaniak [7] have presented generalizations of an idea for continuous control of chaos, proposed by Pyragas [8], for the aim of synchronizing chaotic systems. Continuous control methods have proven to be useful to achieve synchronization in a variety of experimental systems which include electric circuits [9], diode resonators [10], and an yttrium iron garnet film in ferromagnetic resonance [11]. Moreover there are attempts to apply them to the theoretical analysis of blocking phenomena in meteorological systems [12].

More recently the present author [13], using the original Pecora and Carroll driving scheme [1], has reported the existence of two synchronization-like behaviors of a response under nonlinear driving: the amplification (or re-

duction) of the drive attractor, and its reproduction in a region of phase space out of where the stable attractor lies. The study of these phenomena under the Pecora and Carroll method [13] has shown that: (i) these particular behaviors are related to some special symmetries in the systems involved, (ii) the degree of amplification or displacement is determined by the systems initial conditions, and (iii) the stability of the synchronization-like behavior obtained is not asymptotic, but uniform. This has been later observed in computer experiments by Matías *et al.* [14] using the coupling method of their own [3] which is a Pecora and Carroll like method too.

The change of size of the attractor or its displacement in phase space appear promising as they enrich the possibilities of chaotic driving as a tool for practical and scientific applications, and for theoretical analysis. Therefore their study will be expanded in the present article by considering the case of a continuous control method. It will be shown here that amplification and displacement of chaotic attractors can be obtained using continuous control, if the symmetry properties quoted above are present, and that the behaviors obtained differ from their counterparts under Pecora and Carroll like methods in two significant issues: (i) the degree of amplification or displacement can be tuned from the synchronization arrangement, instead of being given by the initial conditions, and (ii) the stability of the response trajectories can be made to be asymptotic, instead than uniform. Therefore these phenomena can be seen as particular cases of the generalized synchronization defined by Rulkov *et al.* [15] and studied by several authors [16–20].

The contents of the paper are arranged as follows. In Section 2, it is defined the type of symmetric chaotic systems that allow amplification and displacement, and in

^a e-mail: jgm@hermes.ffn.ub.es

Section 3 schemes of continuous control to achieve asymptotically stable behaviors will be presented. Then follow three sections which contain a numerical study of two particular models which illustrate the distinctive properties of these generalized synchronization phenomena under continuous control. In Section 4, the systems studied are presented, and the stability of the generalized synchronization behaviors is studied, in Section 5 it is shown how the magnitude of the amplification or displacement observed can be tuned, and in Section 6 it is studied the effect of imperfections in the experimental arrangement on the behaviors observed. Finally, Section 7 includes a summary of the results obtained and some concluding remarks.

2 Symmetric systems

Let us assume that we have a chaotic system that can be described by a set of n variables, $\mathbf{x} = (x_1, x_2, \dots, x_n)$, with a dynamical behavior governed by a set of n non-linear autonomous differential equations

$$\frac{d\mathbf{x}}{dt} = \mathbf{f}(\mathbf{x}). \quad (1)$$

When let to itself, the trajectory followed in phase space will drop on a strange attractor which is a fractal set of points bounded in some region of the n -dimensional phase space.

In this article, it will be studied the case in which there are some transformations of coordinates, $T_{\mathbf{P}}$, that act only on some of the variables, \mathbf{w} , leaving the remainder unchanged. Therefore, the set of variables \mathbf{x} is divided in two subsets

$$\mathbf{x} = \begin{pmatrix} \mathbf{v} \\ \mathbf{w} \end{pmatrix} \quad (2)$$

with respective dimensions l and m , being $l + m = n$, so that the coordinate transformations act on the m coordinates \mathbf{w} , while the remainder \mathbf{v} coordinates are not affected. Then, the dynamical equation are rewritten as

$$\frac{d\mathbf{v}}{dt} = \mathbf{g}(\mathbf{v}, \mathbf{w}) \quad (3)$$

$$\frac{d\mathbf{w}}{dt} = \mathbf{h}(\mathbf{v}, \mathbf{w}) \quad (4)$$

being

$$\mathbf{f}(\mathbf{x}) = \begin{pmatrix} \mathbf{g}(\mathbf{v}, \mathbf{w}) \\ \mathbf{h}(\mathbf{v}, \mathbf{w}) \end{pmatrix}. \quad (5)$$

In particular, given this decomposition, the \mathbf{w} subsystem will be attracted to a set of points bounded in some region of its m -dimensional subspace.

The set of transformations of coordinates $T_{\mathbf{P}}(\mathbf{w}) \equiv \mathbf{w}^*$ have the following properties:

(i) All have the same functional form, being given each particular transformation by the values of a set of parameters $\mathbf{P} = (P_1, P_2, \dots, P_q)$ which are real numbers that

change continuously in a given interval, $P_i \in [a_i, b_i]$, such that $0 \in [a_i, b_i]$.

(ii) If the identity is denoted as \mathbf{I} , then

$$\lim_{\mathbf{P} \rightarrow \mathbf{0}} T_{\mathbf{P}} = \mathbf{I}. \quad (6)$$

(iii) They are continuous in the sense that

$$\lim_{|\mathbf{P} - \mathbf{P}'| \rightarrow 0} |T_{\mathbf{P}}(\mathbf{w}) - T_{\mathbf{P}'}(\mathbf{w})| = 0 \quad (7)$$

for all points of the \mathbf{w} subsystem attractor.

(iv) Under anyone of these transformations equations (4) remain unchanged; *i.e.*, the following equation holds

$$\frac{d\mathbf{w}^*}{dt} = \mathbf{h}(\mathbf{v}, \mathbf{w}^*). \quad (8)$$

Two particular transformations of that type will be studied here. I will call the first an amplitude transformation, it is defined by $T_{(A-1)}(\mathbf{w}) \equiv A \mathbf{w}$, and depends on an amplitude factor A which is a positive real number. The second will be called displacement transformation, it is defined by $T_{\mathbf{D}}(\mathbf{w}) \equiv \mathbf{w} + \mathbf{D}$, and depends on the m components of the translations vector, \mathbf{D} .

3 Continuous control

In the method for synchronization of chaotic systems proposed by Ding and Ott [6], the system described by variables \mathbf{v} and \mathbf{w} , and governed by equations (3, 4) is meant to be the drive. The response system is described by variables \mathbf{v}' and \mathbf{w}' which are copies of \mathbf{v} and \mathbf{w} , and evolve under the dynamical law

$$\frac{d\mathbf{v}'}{dt} = \mathbf{g}'(\mathbf{w}, \mathbf{v}', \mathbf{w}') \quad (9)$$

$$\frac{d\mathbf{w}'}{dt} = \mathbf{h}'(\mathbf{w}, \mathbf{v}', \mathbf{w}') \quad (10)$$

with \mathbf{w} acting as the drive signal, and the functions \mathbf{g}' and \mathbf{h}' such that they become those of the drive when both systems are synchronized; that is,

$$\mathbf{g}'(\mathbf{w}, \mathbf{v}', \mathbf{w}') \rightarrow \mathbf{g}(\mathbf{v}, \mathbf{w}) \quad (11)$$

$$\mathbf{h}'(\mathbf{w}, \mathbf{v}', \mathbf{w}') \rightarrow \mathbf{h}(\mathbf{v}, \mathbf{w}) \quad (12)$$

when $\mathbf{v}' \rightarrow \mathbf{v}$ and $\mathbf{w}' \rightarrow \mathbf{w}$.

Possible choices for \mathbf{g}' and \mathbf{h}' are

$$\mathbf{g}'(\mathbf{w}, \mathbf{v}', \mathbf{w}') = \mathbf{g}(\mathbf{v}', \mathbf{w}') + \tilde{\eta}(\mathbf{w} - \mathbf{w}') \quad (13)$$

$$\mathbf{h}'(\mathbf{w}, \mathbf{v}', \mathbf{w}') = \mathbf{h}(\mathbf{v}', \mathbf{w}') + \tilde{\gamma}(\mathbf{w} - \mathbf{w}') \quad (14)$$

being $\tilde{\gamma}$ and $\tilde{\eta}$ matrices of adjustable parameters that measure the strength of the coupling between drive and response. Under this particular selection of the functions \mathbf{g}' and \mathbf{h}' , this method is a generalization of the case of synchronization of chaos studied by Kapitaniak [7], using

the technique for control of chaos by means of continuous self-controlling feed-back proposed by Pyragas [8].

If the same initial conditions are chosen for drive and response, $\mathbf{v}'(0) = \mathbf{v}(0)$ and $\mathbf{w}'(0) = \mathbf{w}(0)$, the two systems will evolve in synchrony in the sense that, $\mathbf{v}'(t) = \mathbf{v}(t)$ and $\mathbf{w}'(t) = \mathbf{w}(t)$ for $t > 0$. For this synchronization to be asymptotically stable, the largest conditional Lyapunov exponent for the system evolving under equations (9, 10) has to be negative. In this case, this conditional Lyapunov exponent is defined by

$$\Lambda = \lim_{t \rightarrow \infty} \frac{1}{t} \ln \frac{|\delta \mathbf{x}(t)|}{|\delta \mathbf{x}(0)|} \quad (15)$$

being $\delta \mathbf{x} \equiv |\mathbf{v}' - \mathbf{v}| + |\mathbf{w}' - \mathbf{w}|$ an infinitesimal distance between the two systems.

A major advantage of this method is the availability of practically infinite choices for the functions \mathbf{g}' and \mathbf{h}' . Combined with the possibility of setting the numerical values of the coupling parameters, this allows one to obtain asymptotically stable synchronism for almost any system. This possibility has proven to be feasible in the context of the regular synchronization of chaotic systems ($\Delta \mathbf{x} \equiv |\mathbf{x}' - \mathbf{x}| \rightarrow 0$) in a variety of particular cases studied by different authors [6,7,21].

When dealing with chaotic systems bearing the symmetries described in Section 2, this control method can be modified to obtain asymptotically stable amplifications of a part of an attractor, or asymptotically stable motion of the response in a region displaced from the stable attractor. To achieve this the system \mathbf{h}' has to be constructed from the symmetric part of the non-linear system, and the drive signal has to be \mathbf{w} . Moreover $T_{\mathbf{P}}$ has to enter the definition of \mathbf{g}' and \mathbf{h}' in such a way that these functions reduce to those of the drive when transitorities have fallen down; that is,

$$\mathbf{g}'(\mathbf{w}, \mathbf{v}', \mathbf{w}') \rightarrow \mathbf{g}(\mathbf{v}, \mathbf{w}) \quad (16)$$

$$\mathbf{h}'(\mathbf{w}, \mathbf{v}', \mathbf{w}') \rightarrow \mathbf{h}[\mathbf{v}, T_{\mathbf{P}}(\mathbf{w})] \quad (17)$$

when $\mathbf{v}' \rightarrow \mathbf{v}$ and $\mathbf{w}' \rightarrow T_{\mathbf{P}}(\mathbf{w})$ for a fixed \mathbf{P} .

A possible arrangement can be obtained by a modification of a coupling scheme of the type given by equations (13, 14). Then, for the amplitude transformation, the particular choice for \mathbf{g}' and \mathbf{h}' is modified to

$$\mathbf{g}'(\mathbf{v}, \mathbf{v}', \mathbf{w}') = \mathbf{g}(\mathbf{v}', \mathbf{w}'/\alpha) + \tilde{\eta}(\alpha \mathbf{w} - \mathbf{w}') \quad (18)$$

$$\mathbf{h}'(\mathbf{v}, \mathbf{v}', \mathbf{w}') = \mathbf{h}(\mathbf{v}', \mathbf{w}') + \tilde{\gamma}(\alpha \mathbf{w} - \mathbf{w}') \quad (19)$$

where α is a real and positive tuning parameter used to select the degree of amplification which is measured by A . In the same way, for the displacement transformation, a particular proper choice will be

$$\mathbf{g}'(\mathbf{v}, \mathbf{v}', \mathbf{w}') = \mathbf{g}(\mathbf{v}', \mathbf{w}' - \rho) + \tilde{\eta}[(\rho + \mathbf{w}) - \mathbf{w}'] \quad (20)$$

$$\mathbf{h}'(\mathbf{v}, \mathbf{v}', \mathbf{w}') = \mathbf{h}(\mathbf{v}', \mathbf{w}') + \tilde{\gamma}[(\rho + \mathbf{w}) - \mathbf{w}'] \quad (21)$$

where ρ is a vector of tuning parameters used to select the displacement vector \mathbf{D} in the proper subspace. In practice, there is no need to inject all the variables \mathbf{w} of the drive

in the response. This will be shown in Sections 4–6 by means of the study of some particular cases in which only one of the components of one the matrices of coupling parameters, $\tilde{\eta}$ or $\tilde{\gamma}$, is no null.

The comments given in the third paragraph of this section for synchronization, can be directly translated to amplification and displacement. In particular, if the initial condition for the response is $\mathbf{v}'(0) = \mathbf{v}(0)$ and $\mathbf{w}'(0) = T_{\mathbf{P}}[\mathbf{w}(0)]$, the two systems will evolve in a generalized synchronization state in the sense that, $\mathbf{v}'(t) = \mathbf{v}(t)$ and $\mathbf{w}'(t) = T_{\mathbf{P}}[\mathbf{w}(t)]$ for $t > 0$; and, if the largest conditional Lyapunov exponent, Λ , is negative we can have asymptotically stable amplification or displacement of the attractor. Therefore, the stability properties in this case will be determined by the maximum Lyapunov exponent of the subsystem described by equations (9, 10) computed for $\mathbf{P} = 0$.

4 Systems studied and stability

An appropriate model to study the amplification is the Lorenz model [22] described by

$$\dot{X} = \sigma(Y - X) \quad (22)$$

$$\dot{Y} = (R - Z)X - Y \quad (23)$$

$$\dot{Z} = XY - BZ \quad (24)$$

because the equations for X and Y are invariant under an amplitude transformation $T_{(A-1)}(X, Y) \equiv (AX, AY)$. The particular response system studied here is

$$\dot{X}' = \sigma(Y' - X') \quad (25)$$

$$\dot{Y}' = (R - Z')X' - Y' + \gamma_{y,y}(\alpha Y - Y') \quad (26)$$

$$\dot{Z}' = \frac{X'Y'}{\alpha^2} - BZ' \quad (27)$$

being α a tuning parameter for the amplitude of the response, and $\gamma_{y,y}$ a single constant that measures the stiffness of the coupling, and has to be chosen to obtain asymptotically stable behavior. For simplicity, the notation $\gamma \equiv \gamma_{y,y}$ will be used in the remainder of the paper. The numerical results for this model have been obtained for the parameter values $\sigma = 16$, $R = 45.92$, and $B = 4$, using a fourth-order Runge-Kutta algorithm with a time step of 0.003.

The displacement has been studied in the Double-Scroll [23] which is given by:

$$\dot{X} = \alpha[Y - X - F(X)] \quad (28)$$

$$\dot{Y} = X - Y + Z \quad (29)$$

$$\dot{Z} = -\beta Y \quad (30)$$

being

$$F(X) = bX + \frac{1}{2}(a-b)[|X+1| + |X-1|]. \quad (31)$$

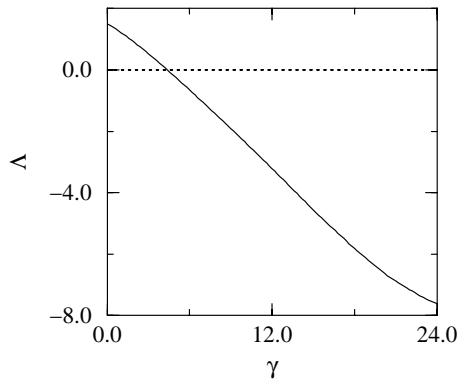


Fig. 1. Largest conditional Lyapunov exponent as a function of the coupling parameter γ for the Lorenz model. The dashed lines signal the borders between positive and negative exponents.

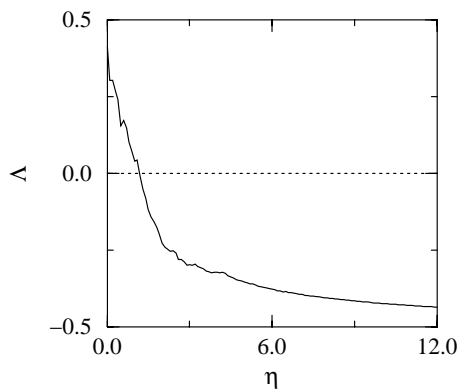


Fig. 2. Same that Figure 1 for the Double-Scroll and the coupling parameter η .

The equations for X and Z are invariant under a transformation $T_D(Z) \equiv Z + D$; therefore, one may obtain a displacement of the attractor in the Z direction using as the response a system such as

$$\dot{X}' = \alpha [Y' - X' - F(X')] \quad (32)$$

$$\dot{Y}' = X' - Y' + (Z' - \rho) - \eta_{y,z} [(\rho + Z) - Z'] \quad (33)$$

$$\dot{Z}' = -\beta Y' \quad (34)$$

being ρ the tuning parameter, and $-\eta_{y,z}$ the stiffness adjustable parameter used to achieve asymptotically stable behavior when the Z signal is injected in the response. In the remainder of the article the simpler notation $\eta \equiv -\eta_{y,z}$ will be used. The results presented here have been obtained for $\alpha = 10$, $\beta = 14.87$, $a = -1.27$ and $b = -0.68$, with a fourth-order Runge-Kutta algorithm with a time step 0.02.

I have computed the largest conditional Lyapunov exponent, Λ , for these systems at the parameter values said above. Because \mathbf{g}' and \mathbf{h}' have as additional parameters the stiffness constants, γ and η , the conditional Lyapunov

exponents have to be dependent on these parameters. The results obtained for Λ as a function of γ (for $\alpha = 1$) and of η (for $\rho = 0$), are displayed in Figure 1 for the Lorenz model, and Figure 2 for the Double-Scroll. They show that it is possible to find a threshold for the coupling parameter above which one has a negative conditional Lyapunov exponent, and then asymptotically stable phenomena of amplification or displacement. This threshold holds for any values of α or ρ , because of the invariance properties of the equations of motion. In the remainder of the paper the values of $\gamma = 12.0$ and $\eta = 6.0$, that warrant asymptotic stability, will be used to study this type of driving.

5 Tuning the desired behavior

To observe the amplification of the attractor, in the Lorenz model, and the displacement, in the Double-Scroll, the equations of motion given in Section 4 have been integrated in each case. Various sets of values of γ and α for the Lorenz model, and of η and ρ for the Double-Scroll, as well as different sets of values for the initial conditions have been tested. The corresponding phenomena have been monitored both, by means of plots of the time evolution of the drive and response variables and by parametric plots of the variables of the response *versus* the variables of the drive. This last type of plots appear as straight lines when both signals evolve in perfect synchrony, the amplification of the signal, A , is measured by the slope of the straight line, and the displacement, D , by its ordinate in the origin. Representative plots of the results obtained are given in Figures 3, 4, and 5.

The amplification of the X signal for the Lorenz attractor for $\alpha = 5$ is displayed in Figure 3a where it is shown how, after a short transitory, the response trajectory closely reproduces the drive signal amplified 5 times. The same can be seen in the parametric plot (Fig. 4) for the Y signal. A case of displacement of the attractor for the Double-Scroll, using $\rho = +10$ is shown in Figures 3b and 5. The expected behavior is appreciated in both plots after transitories die. The degree of amplification or displacement, in both cases, is controlled by the values of α or ρ . The main effect of initial conditions is on the duration and complexity of the transitories that precede the settlement of the amplified or displaced evolution. There may be, however, some additional influence of the initial conditions. This is because initial conditions for the response that are far from the trajectory tuned to be followed may give rise to unstable, divergent evolutions of the response. This was found to happen in the Lorenz model. Therefore, for these systems, the initial conditions for the response have to be chosen in a region of phase space around the one where the response is expected to evolve. In practice, this is not an stringent condition.

In Figure 6 it is illustrated how the continuous control method is efficient to obtain the desired amplification or displacement of the attractor. There the dependence of A with α , for the Lorenz model, and D with ρ for the Double-Scroll, obtained in a series of numerical integrations of the equations of motion with initial condition

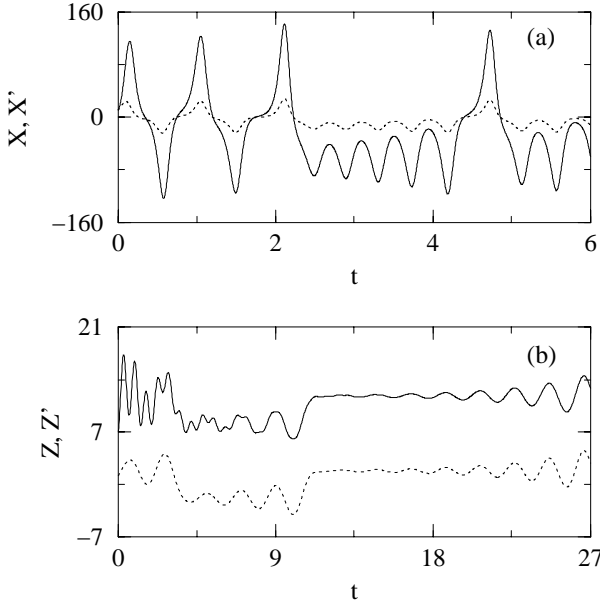


Fig. 3. Amplification and displacement obtained by means of continuous control. (a) Time evolution of the X signal for the drive (dashed line) and the response (solid line) for the Lorenz model, using $\gamma = 12$ and $\alpha = 5$ and (b) time evolution of the Z signal for the drive (dashed line) and the response (solid line) for the Double-Scroll, using $\eta = 6.0$ and $\rho = 10$.

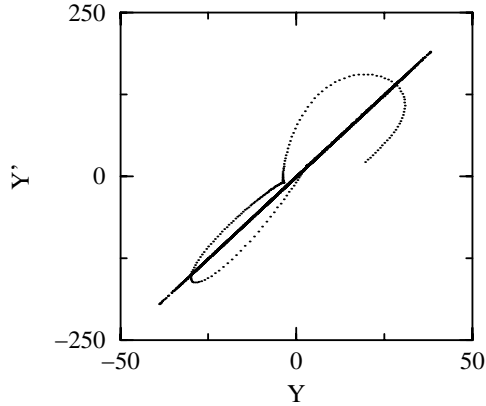


Fig. 4. Parametric plot of the Y signal for the Lorenz model, using $\gamma = 12$ and $\alpha = 5$.

randomly choose for each point are displayed. For the Lorenz model, each point in Figure 6 represents the value observed for A for an evolution computed for a given value or the parameter α . The initial conditions used for any point are unique to this point: (X_0, Y_0, Z_0) was randomly chosen as a point in the stable attractor for the drive, and (X'_0, Y'_0, Z'_0) was randomly selected within a parallelepiped centered at the point $(0, 0, \Delta Z)$ and with edges of length $\alpha 2\Delta X$, $\alpha 2\Delta Y$ and $2\Delta Z$, being ΔX , ΔY and ΔZ the amplitudes of the fluctuations of the signals X , Y and Z of the drive system. For the Double-Scroll, each point in Figure 6 represents the observed value for D for

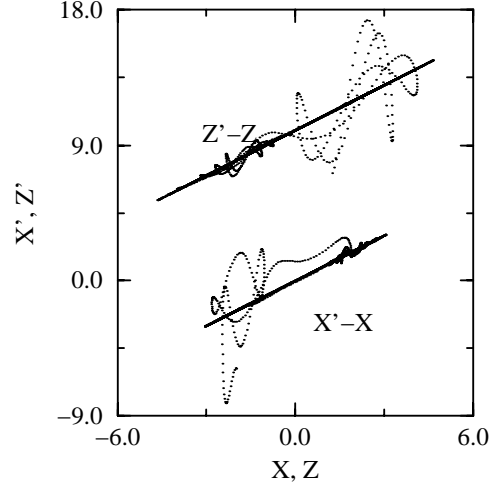


Fig. 5. Parametric plots of the X and Z signals for the Double-Scroll, using $\eta = 6.0$ and $\rho = 10$.

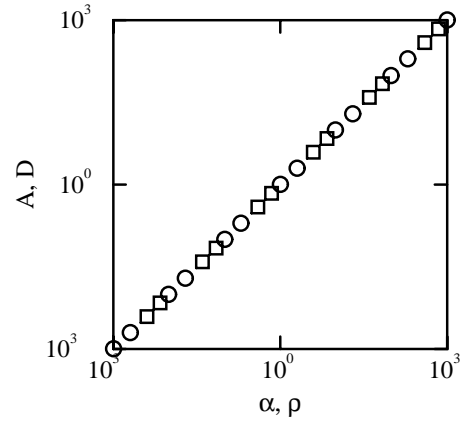


Fig. 6. Dependence of the amplification, A , or displacement, D , effectively obtained for the response as functions of the turning parameters, α or ρ , used in each case. In this figure the function $A(\alpha)$ is indicated by circles, and the function $D(\rho)$ is indicated by squares.

a single evolution made for a given value of the parameter ρ . The initial conditions for each run have been chosen in a similar manner: (X_0, Y_0, Z_0) as a point in the stable attractor for the drive, and (X'_0, Y'_0, Z'_0) within a parallelepiped centered at the unstable fixed point $(0, 0, 0)$ and with edges of length $2\Delta X$, $2\Delta Y$ and $2\Delta Z$, with ΔX , ΔY and ΔZ the amplitudes of the fluctuations of the drive signals. The points aligned along straight lines illustrate a distinctive feature of the continuous control method: the degree of amplification, A , or the displacement, D , obtained can be selected as desired by choosing appropriate values for the turning parameters, α or ρ . Once these parameters are fixed on, the response trajectory, after some transients die, will reproduce a copy of the drive attractor amplified by a factor $A = \alpha$, or displaced an amount $D = \rho$ in the Z direction.

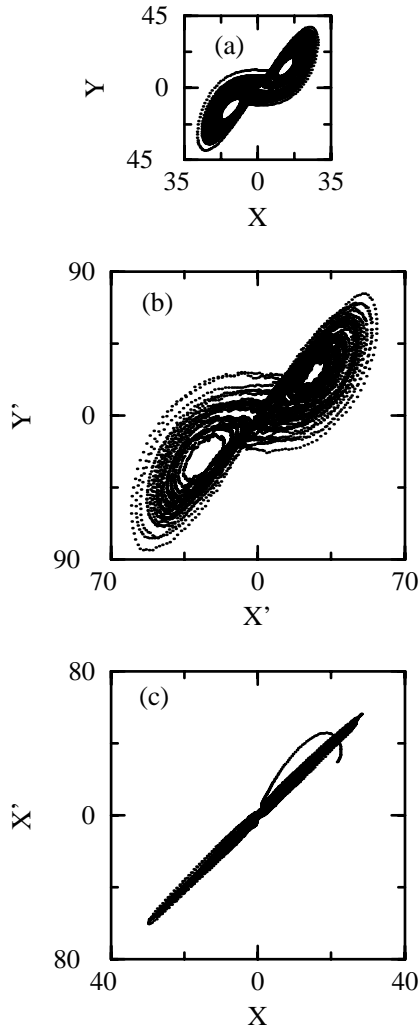


Fig. 7. (a) Drive attractor trajectory, (b) trajectory followed by the response and (c) parametric plot for the Lorenz model under a noisy continuous control drive scheme. The observational time window spans 10000 time steps and the parameters used are $\gamma = 12$, $\alpha = 2$, and $\sigma_Y = 0.10$

6 External noise and parameter mismatch

To study the robustness of the response trajectories in the presence of external noise, a series of time evolutions have been performed adding a Gaussian white noise to the drive signal. Therefore, the signal effectively injected in the response was $\mathbf{w}(t) + \delta_t$, being δ_t a small quantity whose values are randomly distributed along a Gaussian function centered at zero. The strength of this noise is measured by the dispersion in the distribution of δ_t , σ , which, measured in units of the amplitude of the controlling signal, is the control parameter in this study. Plots of the response trajectories and parametric plots are displayed in Figure 7 for the Lorenz model and in Figure 8 for the Double-Scroll. For both models, below certain level of noise, one always obtains a response trajectory that accurately reproduces the drive attractor amplified (shrunken) or displaced, and

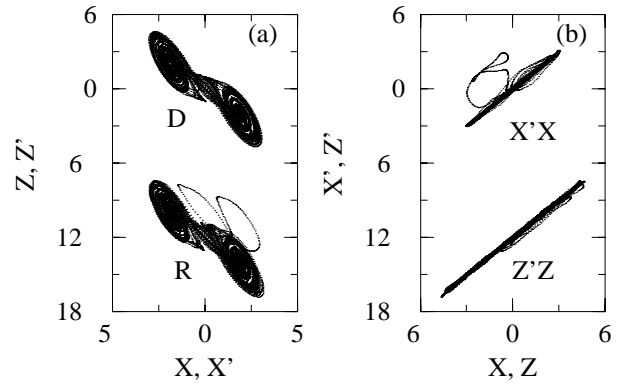


Fig. 8. (a) Trajectories followed by the response, and (b) parametric plots for the Double-Scroll under a noisy continuous control drive scheme. The observational time window spans 10000 time steps and the parameters used are $\eta = 6.0$, $\rho = -12$, and $\sigma_Z = 0.1$.

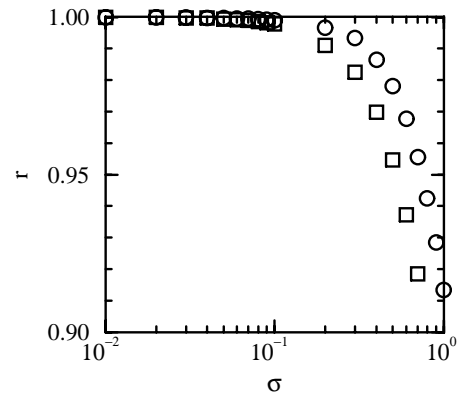


Fig. 9. Effect of external noise in the accuracy of the synchronization when the continuous control of chaos method is used measured by its effect on the correlation coefficient, r , of the fit to a straight line of $X' = X'(X)$ for amplification (circles) and $Z' = Z'(Z)$ for displacement (squares).

as that level of noise is increased the response trajectories and parametric plots gradually become blurred versions of the free noise case as correspond to a case of asymptotic stability. It is to be noted that the noise level in Figures 7 and 8 is quite large (10 per cent of the amplitude of the drive signal), what illustrates how efficient a continuous control method can be to maintain the response system close to the desired trajectory. To have an overall view of the effect of noise I have computed the correlation coefficient, for the fit of straight lines to the appropriate parametric functions, $X' = X'(X)$ for the Lorenz Model and $Z' = Z'(Z)$ for the Double-Scroll, for the different values of the noise amplitude. The results, shown in Figure 9 illustrate how a perfect fit becomes gradually lost only when the noise amplitude overcomes a size as large as 0.1 of the amplitude of the signal.

Some calculations have been done to study the effect of the parameter mismatch between drive and response. This is measured by $\varepsilon_p \equiv (p' - p)/p$, being p and p' the

parameter values of the drive and the response, respectively. In this case one obtains a response behavior that smoothly evolves from the one corresponding to $\varepsilon_p = 0$, to another in which the response trajectory is still amplified or displaced, but somehow deformed. A couple of examples of response trajectories for large parameter mismatch are displayed in Figure 10. For the Lorenz model and σ -parameter mismatch one obtains (Fig. 10a) a copy of the attractor which is an amplified and deformed version of the well-known Lorenz attractor (it appears compressed in the direction perpendicular to the main diagonal). For the Double-Scroll, shown here for α parameter mismatch (Fig. 10b), one obtains that the response trajectory is such that Z' reproduces a displaced copy of Z , while X' evolves in a complicated way giving rise to a whole response trajectory that looks like a (displaced) deterministic attractor that resembles an split version of the original.

In the particular implementations of the control scheme given by equations (25–27) for the Lorenz model and by equations (32–34) for the Double-Scroll, new parameters have been included to fulfill the conditions imposed by equations (16, 17). These are $\mu \equiv 1/\alpha^2$ in the term $X'Y'$ of equation (27), (*i.e.*, $\dot{Z}' = \mu X' Y' - B Z'$) and $\nu \equiv \rho$ in the term $(Z' - \rho)$ of equation (33) (*i.e.*, $\dot{Y}' = X' - Y' + (Z' - \nu) - \eta_{y,z}\{(\rho + Z) - Z'\}$). This introduces a new type of parameter mismatch that, in a practical device, may occur within the response subsystem. It is measured by $\varepsilon_p \equiv (p' - p)/p$, being p the value of the parameter for zero mismatch and p' its actual value. I have performed tests as those described in the above paragraph for these new parameters μ and ν . The results show that such mismatches do not compromise the synchronization with amplification or displacement. This is illustrated in Figure 11, where there are displayed parametric plots for $\alpha = 2$ and ten percent mismatch in μ ($\varepsilon_\mu = 0.1$) for the Lorenz model, and $\rho = 10$ and one hundred per cent mismatch in ν ($\varepsilon_\nu = 1.0$) for the Double-Scroll. For amplification, the effect of such mismatch is qualitatively similar to the effect of external noise shown in Figure 7c. For displacement, ν competes against ρ to modify the degree of displacement in an amount that is one order of magnitude smaller than ε_ν , which has been chosen very large in Figure 11b to make its effect perceptible. Anyway, these results, together with those in the above paragraph, show that the response behavior is stable against parameter mismatch.

7 Concluding remarks

In summary, it has been shown that by using continuous control on chaotic systems that exhibit invariance properties under continuous transformations, one can obtain partial amplification of the attractor or displacement of it to a region of phase space where the original system is not stable. The distinctive features of these phenomena under continuous control are: (i) the stability of such orbits can be made to be asymptotic; therefore, one can properly talk about generalized synchronization [15], and

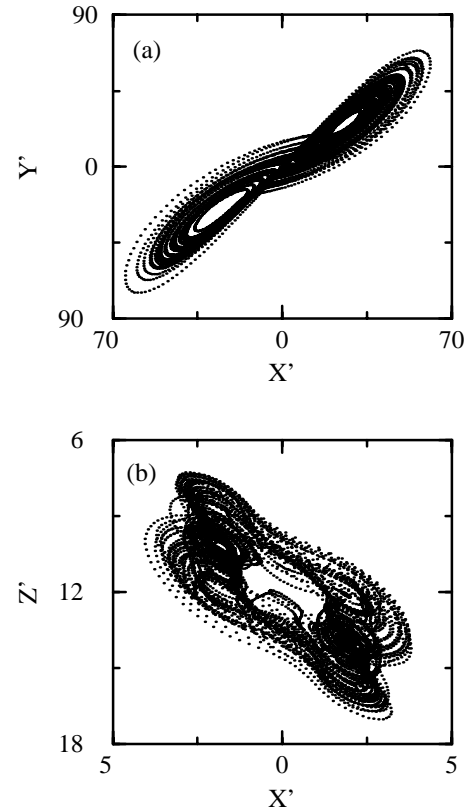


Fig. 10. Trajectory followed by the response for the (a) Lorenz system, under continuous control and large σ parameter mismatch ($\varepsilon_\sigma = 1$), and (b) for the Double-Scroll under continuous control and large α parameter mismatch ($\varepsilon_\alpha = 1$). Both plots are for times when the transitories have died out.

(ii) the degree of amplification and displacement can be tuned by adjusting the controlling scheme. A numerical study of these phenomena has been performed for two mathematical models, exhibiting one of them the symmetry appropriate for amplification (the Lorenz model), and the other the symmetry appropriate for displacement (the Double-Scroll). For continuous control, and perfect coupling, it has been shown that it is possible to design driving schemes that allow to obtain asymptotically stable behavior with negative conditional Lyapunov exponents. The degree of amplification and displacement was indeed found tunable by changes in the parameters of the controlling arrangement. Computer simulations under noisy situations or system parameter mismatch have shown that the behavior of the response is particularly robust against imperfections in the control arrangement. This supports the idea that such phenomena are able to be reproduced in the laboratory or observed in nature.

The behaviors of chaotic systems under continuous control studied in the present article are different than the synchronization behavior that has been widely studied in the literature. Therefore, they represent an enrichment of the tools available in several fields of science and technology. Technical applications of the ideas and results presented in this paper might occur in the field of communications [24], where there are problems that have to

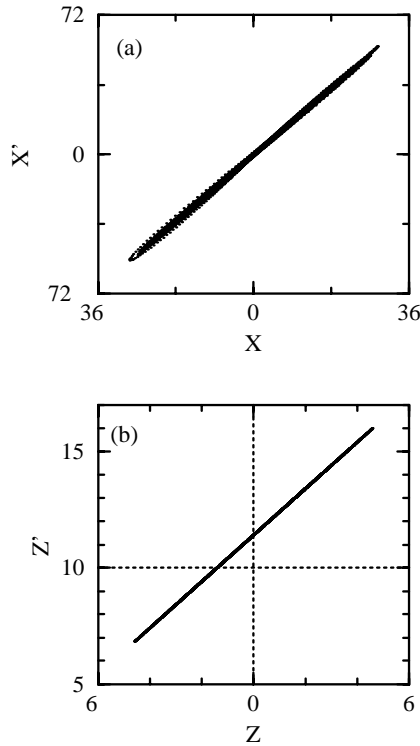


Fig. 11. Parametric plots for (a) the Lorenz model for $\alpha = 2$ and μ parameter mismatch ($\varepsilon_\mu = 0.1$), and (b) for the Double-Scroll for $\rho = 10$ and ν parameter mismatch ($\varepsilon_\nu = 1.0$). The broken lines are guides to the eye. Both plots are for times when the transitorities have died out.

be addressed in issues such as signal attenuation along a line [25], and safety [26, 27]. The results presented here on controlling the amplitude or position of chaotic attractors might allow new approaches to these issues.

Neurobiology appears as a possible field for application too. For example, the analyses of multigrid electroencephalograms performed on several neural systems has demonstrated two relevant facts [28–32]: (i) the local electrical activity can be described by means of low dimensional chaotic systems, and (ii) the global behavior is characterized by spatial patterns, which are defined by the different amplitudes of the signals measured at each electrode. The results presented in this article appear as possible tools to model behaviors of that kind by means of networks of low-dimensional chaotic systems bearing the symmetries appropriate to exhibit amplification.

This research has been supported by DGICYT, through project PB96-0392.

References

1. L.M. Pecora, T.L. Carroll, Phys. Rev. Lett. **64**, 821 (1990).
2. T.L. Carroll, L.M. Pecora, Physica D **67**, 126 (1993).
3. J. Güémez, M.A. Matías, Phys. Rev. E **52**, R2145 (1995).
4. L. Kocarev, U. Parlitz, Phys. Rev. Lett. **74**, 5028 (1995).
5. T.L. Carroll, J.F. Heagy, L.M. Pecora, Phys. Rev. E **54**, 4676 (1996).
6. M. Ding, E. Ott, Phys. Rev. E **49**, R945 (1994).
7. T. Kapitaniak, Phys. Rev. E **50**, 1642 (1994).
8. K. Pyragas, Phys. Lett. A **170**, 421 (1992).
9. Y.H. Yu, K. Kwak, T.K. Lim, Phys. Lett. A **191**, 233 (1994).
10. T.C. Newell, P.M. Alsing, A. Gavrielides, V. Kovanis, Phys. Rev. Lett. **72**, 1647 (1994).
11. D.W. Peterman, M. Ye, P.E. Wigen, Phys. Rev. Lett. **74**, 1740 (1995).
12. A. Stefanski, T. Kapitaniak, J. Brindley, Physica D **98**, 594 (1996).
13. J.M. González-Miranda, Phys. Rev. E **53**, R5 (1996).
14. M.A. Matías, J. Güémez, C. Martín, Phys. Lett. A **226**, 264 (1997).
15. N.F. Rulkov, M.M. Sushchik, L.S. Tsimring, H.D.I. Abarbanel, Phys. Rev. E **51**, 980 (1995).
16. N.F. Rulkov, M.H. Sushchik, Phys. Lett. A **214**, 145 (1996).
17. H.D.I. Abarbanel, N.F. Rulkov, M.M. Sushchik, Phys. Rev. E **53**, 4528 (1996).
18. J.M. González-Miranda, Phys. Rev. E **53**, 5656 (1996).
19. K. Pyragas, Phys. Rev. E **54**, R4508 (1996).
20. A. Kittel, J. Parisi, K. Pyragas, Physica D **112**, 459 (1998).
21. G. Malescio, Phys. Rev. E **53**, 2949 (1996).
22. E.N. Lorenz, J. Atmos. Sci. **20**, 130 (1963).
23. T. Matsumoto, L.O. Chua, M. Komuro, IEEE Trans. CAS **32**, 797 (1985).
24. K.M. Cuomo, A.V. Oppenheim, Phys. Rev. Lett. **71**, 65 (1993).
25. T.L. Carroll, Phys. Rev. E **53**, 3117 (1996).
26. K.M. Short, Int. J. Bifurc. Chaos **4**, 959 (1994).
27. G. Pérez, H.A. Cerdeira, Phys. Rev. Lett. **74**, 1970 (1995).
28. W.J. Freeman, W. Schneider, Psychophysiol. **19**, 44 (1982).
29. B. Baird, Physica D **22**, 150 (1986).
30. W.J. Freeman, IEEE Trans. CAS **35**, 781 (1988).
31. W.J. Freeman, Physica D **75**, 150 (1994).
32. R. Friedrich, C. Uhe, Physica D **98**, 171 (1996).